



Net and gross oxygen production from O₂/Ar, ¹⁷O/¹⁶O and ¹⁸O/¹⁶O ratios

Boaz Luz*, Eugeni Barkan

The Institute of Earth Sciences, The Hebrew University of Jerusalem, Jerusalem 91904, Israel

ABSTRACT: In aquatic systems, variations in the O₂/Ar ratio and in the ¹⁷O anomaly (¹⁷Δ, calculated from ¹⁷O/¹⁶O and ¹⁸O/¹⁶O) are affected by both physical and biological processes. Laboratory observations suggest that ¹⁷Δ is independent of respiration rate, in contrast to the O₂/Ar ratio. This makes it possible to determine gross O₂ production from measurements of ¹⁷O/¹⁶O and ¹⁸O/¹⁶O of dissolved O₂, while the O₂/Ar ratio can be applied to estimate net O₂ production. We demonstrate how biological and physical forcing modifies the O₂/Ar ratio and ¹⁷Δ during the day and at night in a coral reef near Eilat. This field study confirmed our hypothesis that ¹⁷Δ of dissolved O₂ (¹⁷Δ_{dis}) is affected by photosynthesis, ocean dynamics and air–water gas exchange, but not by respiration. We also show, for the first time, a detailed record of ¹⁷Δ responses to biological fluxes and subtropical ocean dynamics on a seasonal scale. The measurements were conducted in the Atlantic Ocean near Bermuda during monthly cruises of the Bermuda Atlantic Time-series Study (BATS) from March 2000 to January 2001. With the formation of the seasonal thermocline, ¹⁷Δ_{dis} significantly increased below the oceanic mixed layer, reflecting the seasonal integration of photosynthesis in the thermocline. Hence, ¹⁷Δ_{dis} accumulation may be used to calculate the overall rate of photosynthesis below the mixed layer. We used the O₂/Ar ratio and ¹⁷Δ_{dis} to estimate net and gross O₂ production (NOP and GOP) and directly compared them with production values derived from ¹⁴C incubations. In general, GOP based on ¹⁷Δ_{dis} was several times greater than production determined via ¹⁴C fixation [P(¹⁴C)], which in turn was somewhat greater than NOP based on the O₂/Ar ratio. The NOP/GOP ratio was 0.08 to 0.21. This implies that the observed high GOP/P(¹⁴C) ratios result mainly from rapid cycling of O₂ between photosynthesis and O₂ uptake mechanisms.

KEY WORDS: Gross production · Net production · Community production · Oxygen isotopes · O₂/Ar ratio · Bermuda Atlantic Time-series Study · Coral reef

Resale or republication not permitted without written consent of the publisher

INTRODUCTION

The metabolic balance between gross primary production and marine community respiration is a major factor affecting the global cycles of carbon and oxygen. For this reason, marine biologists and geochemists have devised different ways of estimating the rates of photosynthesis and respiration. While the basic mechanisms affecting these rates can be studied in small-scale laboratory and field experiments, understanding their manifestation in the sea must take into account the interaction of free living communities with large-scale ocean dynamics. We have previously shown (Luz & Barkan 2000, 2005) that one of the best ways to

investigate the effects of these interactions is by field-scale observations of dissolved O₂ and its 3 isotope species (expressed in the ¹⁷O anomaly, ¹⁷Δ). Together, these 2 parameters can be used to assess net and gross primary productivity as well as community respiration, the latter being the difference between them. Our ¹⁷Δ method has been adopted by other laboratories and used extensively for estimating gross O₂ production (GOP) in different parts of the world ocean (Hendricks et al. 2004, 2005, Juraneck & Quay 2005, Sarma et al. 2005, 2008, Reuer et al. 2007).

A basic premise of our method was that ¹⁷Δ_{dis} is not affected by respiration. However, this assumption was based only on our laboratory experiments. Therefore,

*Email: boaz.luz@huji.ac.il

our first aim in the present study was to go beyond laboratory observations and proceed to large-scale field experiments, to show that $^{17}\Delta$ is indeed not affected by respiration. Towards this goal, we conducted systematic measurements of the O_2/Ar ratio and $^{17}\Delta$ of dissolved O_2 ($^{17}\Delta_{dis}$) in the coral reef reserve near Eilat (Israel), where photosynthesis and respiration have large diel variations.

With the exception of the work by Juranek & Quay (2005), only little attention has been paid to seasonal variations in $^{17}\Delta_{dis}$, and even in that study, depth profiles were measured with low temporal resolution. Yet, much higher resolution is necessary for the estimation of GOP in the seasonal thermocline. Therefore, a second goal of the present study was to show how $^{17}\Delta$ is affected by biological fluxes and ocean dynamics on a seasonal scale. To do this, we monitored the O_2/Ar ratio and $^{17}\Delta_{dis}$ in the Atlantic Ocean near Bermuda during routine cruises conducted as part of the Bermuda Atlantic Time-series Study (BATS) from March 2000 to January 2001. The BATS program was ideal for our purpose because it is carried out at a station where hydrography and biogeochemistry are well known. Moreover, ^{14}C -fixation experiments are routinely done for estimating primary productivity. Thus, the BATS program offered an attractive opportunity for direct comparison of production estimated from the traditional ^{14}C label bottle incubation (*in vitro* method) and estimated with our *in situ* method.

MATERIALS AND METHODS

Biological O_2 supersaturation and net O_2 production (NOP). O_2 saturation in the ocean is defined as $[O_2]/[O_2]_{eq}$, where $[O_2]$ is the observed concentration and $[O_2]_{eq}$ is the equilibrium solubility value. O_2 concentration is affected by both physical (water warming or cooling, barometric pressure variations, and air injection by downward transport of bubbles) and biological (photosynthesis and O_2 respiration) processes. Because the physical properties of O_2 and argon (Ar) are very similar, and Ar has no biological sources or sinks, $\Delta_{phys}[O_2]/[O_2]_{eq} \approx \Delta[Ar]/[Ar]_{eq}$ in the first approximation, where $\Delta_{phys}[O_2]$ and $\Delta[Ar]$ are concentration differences due to addition or removal of O_2 and Ar by physical processes. Thus, measurements of Ar supersaturation can be used to remove physical contributions to O_2 supersaturation (Craig & Hayward 1987, Spitzer & Jenkins 1989).

A useful concept regarding net photosynthetic production is 'biological O_2 supersaturation', $([O_2]/[O_2]_{eq})_{bio}$, which expresses O_2 supersaturation in excess of Ar supersaturation. This was used by Emerson et al. (1991) and Quay et al. (1993) to study biological pro-

ductivity in surface waters of the subarctic Pacific Ocean. Using the same concept, Luz et al. (2002) and Hendricks et al. (2004) calculated 'biological O_2 supersaturation' directly from mass spectrometric measurements of O_2/Ar ratios $[O_2/Ar]_{meas}$ as:

$$([O_2]/[O_2]_{eq})_{bio} = \frac{(O_2/Ar)_{meas}}{(O_2/Ar)_{eq}} = \frac{\delta[(O_2/Ar)_{meas}] + 1}{\delta(O_2/Ar)_{eq} + 1} \quad (1)$$

where $\delta O_2/Ar = (^{32}O_2/^{40}Ar)_{samp}/(^{32}O_2/^{40}Ar)_{ref} - 1$ and the subscripts samp and ref stand for a measured sample and the mass spectrometer reference gas.

Following the above, for the oceanic mixed layer at steady state, NOP can be calculated as in Luz et al. (2002):

$$NOP = k[O_2]_{eq} [(O_2/[O_2]_{eq})_{bio} - 1] \quad (2)$$

where k is the coefficient of air–sea gas exchange ('piston velocity').

Gross O_2 production (GOP). Luz & Barkan (2000) introduced a method for the estimation of GOP from the natural abundance of the 3 stable O_2 isotopes in dissolved O_2 . The basic premise of the triple isotope method is that atmospheric O_2 contains a nonbiological isotope signature. This signature is removed by photosynthesis and can therefore be used to estimate GOP. As discussed by Luz et al. (1999) and Luz & Barkan (2005), the nonbiological signature originates from non-mass-dependent isotope effects of photochemical reactions in the stratosphere. As a result of these reactions, atmospheric O_2 becomes anomalously depleted in ^{17}O . Following Luz & Barkan (2005), excess ^{17}O in dissolved O_2 with respect to atmospheric O_2 is calculated as:

$$^{17}\Delta_{dis} = \ln(\delta^{17}O + 1) - 0.518 \ln(\delta^{18}O + 1) \quad (3)$$

where $\delta^*O = (*R_{smp}/*R_{ref} - 1)$ and its values are reported in δ deviations from the reference gas (atmospheric O_2 , see Barkan & Luz (2003) for detailed discussion); and $*R_{smp}$ and $*R_{ref}$ are the $*O/^{16}O$ ratios in the sample and reference, respectively. The magnitude of $^{17}\Delta$ is always small and, for convenience, it is multiplied by 10^6 and reported in per meg (1 per meg = 0.001 δ). The factor 0.518 is the ratio between the $^{17}O/^{16}O$ and $^{18}O/^{16}O$ isotope effects in ordinary respiration (Luz & Barkan, 2005)—the most widespread O_2 consuming mechanism on Earth. It is important to mention that, in the calculation of $^{17}\Delta$ of dissolved O_2 , the mass-dependent fractionation slope 0.518 should be used and not 0.516. The latter value is correct only for global atmospheric budgets (see Luz & Barkan 2005 for a detailed discussion).

Fig. 1 is a simplified illustration of how photosynthesis, respiration and air–sea gas exchange affect $^{17}\Delta$ of dissolved O_2 ($^{17}\Delta_{dis}$). Assuming a starting point where dissolved O_2 is in gas exchange equilibrium

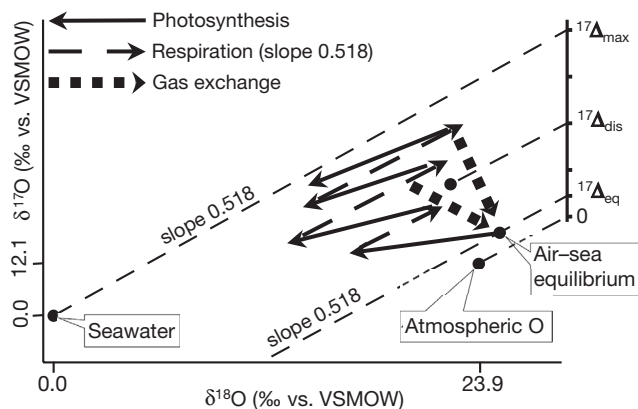


Fig. 1. Schematic illustration (not to scale) showing biological and gas exchange effects on $\delta^{18}\text{O}$, $\delta^{17}\text{O}$ and $^{17}\Delta$ of dissolved O_2 ($^{17}\Delta_{\text{dis}}$). The scale on the right is for $^{17}\Delta_{\text{dis}}$. The $^{17}\Delta_{\text{dis}}$ value of a given point is the intercept of a line with slope 0.518 going through the $^{17}\Delta_{\text{dis}}$ scale. For example, $^{17}\Delta$ of atmospheric O_2 is 0 on that scale. Note that $^{17}\Delta_{\text{dis}}$ increases due to photosynthesis, decreases due to gas exchange, but is not changed by respiration (see text for explanation). The values of $\delta^{18}\text{O}$ and $\delta^{17}\text{O}$ of air O_2 vs. VSMOW (Vienna Standard Mean Ocean Water) are from Barkan & Luz (2005)

with atmospheric O_2 , the $^{17}\Delta_{\text{dis}}$ of such O_2 is defined as $^{17}\Delta_{\text{eq}}$ (Luz & Barkan, 2000). For simplicity, we first consider how photosynthesis alone will modify the isotopic composition of dissolved O_2 . From laboratory experiments (Guy et al. 1993, Helman et al. 2005), we know that O_2 gas produced by photosynthesis has $\delta^{18}\text{O}$ and $\delta^{17}\text{O}$ values close to those in the substrate water. Thus, newly produced O_2 will mix with the existing O_2 and, depending on the extent of photosynthesis, the isotopic composition of the mixture will move towards that of seawater (solid arrows in Fig. 1). We now consider the effect of respiration alone on this mixture. It is known that the ratio of the $^{18}\text{O}/^{16}\text{O}$ and $^{17}\text{O}/^{16}\text{O}$ isotope effects in aquatic organisms is 0.518 (Luz & Barkan 2005). Therefore, the effect of respiration is a change in the composition of dissolved O_2 in Fig. 1 along the dashed arrows with a slope of 0.518. However, because this slope was also chosen in the definition of $^{17}\Delta$ (Eq. 3), respiratory shifts in isotopic composition do not change the $^{17}\Delta_{\text{dis}}$.

In a simple case where ordinary respiration and photosynthesis are the only processes affecting $^{17}\Delta_{\text{dis}}$, and if enough time is allowed, these processes will replace the composition of O_2 at the start with a new one that is affected by biology alone. Luz & Barkan (2000) performed such experiments and showed that the resulting $^{17}\Delta$ at steady state was 249 per meg. We use the term $^{17}\Delta_{\text{max}}$ to designate such O_2 because from this point on, further recycling by photosynthesis and respiration will not increase $^{17}\Delta$. If we now allow only gas exchange, it will shift the composition of dissolved O_2 towards the point where $^{17}\Delta_{\text{dis}} = ^{17}\Delta_{\text{eq}}$.

From this follows that, depending on the ratio of photosynthesis and gas exchange rates, $^{17}\Delta_{\text{dis}}$ moves between 2 lines, both of which have a slope of 0.518. One line goes through seawater composition and the other through a point where $\delta^{17}\text{O}$ and $\delta^{18}\text{O}$ of dissolved O_2 are at equilibrium with atmospheric O_2 . The difference between $^{17}\Delta_{\text{dis}}$ and $^{17}\Delta_{\text{eq}}$ is a measure of the extent to which O_2 in the mixed layer has been replaced by new photosynthetic O_2 .

Based on the above consideration Luz & Barkan (2000) showed that, for a mixed layer in steady state, GOP can be estimated from the following relationship:

$$\text{GOP} = k[\text{O}_2]_{\text{eq}}(^{17}\Delta_{\text{dis}} - ^{17}\Delta_{\text{eq}})/(^{17}\Delta_{\text{max}} - ^{17}\Delta_{\text{dis}}) \quad (4)$$

This approach has been extensively applied for studying GOP in different parts of the world ocean (Hendricks et al. 2004, 2005, Juranek & Quay 2005, Sarma et al. 2005, 2008, Reuer et al. 2007).

Field methods and laboratory measurements. The details of our water sampling procedure are given in Luz et al. (2002). Briefly, seawater was transferred directly from shipboard samplers into pre-evacuated gas extraction vessels (300 ml flasks with Louwers Hapert O-ring stopcocks, containing 1 ml of HgCl_2 saturated solution to prevent biological activity), and the flasks were shipped to the laboratory for further treatment. Sample preparation and mass spectrometry measurements were carried out according to Luz et al. (2002) and Barkan & Luz (2003). The water and headspace in the flask were equilibrated for 24 h at room temperature, and the water was then drawn out of the flasks leaving only headspace gases. Following this, the flasks were connected to a preparation line for the purification of the O_2 -Ar mixture. The $^{18}\text{O}/^{16}\text{O}$ and $^{17}\text{O}/^{16}\text{O}$ ratios in the purified O_2 -Ar mixture were determined by dual inlet mass spectrometry on a multi-collector instrument (Thermo Finnigan Delta^{plus}), which allows simultaneous measurement of m/z 32, 33 and 34 originating from $^{16}\text{O}^{16}\text{O}$, $^{17}\text{O}^{16}\text{O}$, and $^{18}\text{O}^{16}\text{O}$. The O_2/Ar ratio was determined from peak switching between m/z 32 and 40. The analytical errors (SEs of the mean multiplied by Student's *t*-factor for 95% CIs) in $\delta^{18}\text{O}$, $\delta\text{O}_2/\text{Ar}$ and $^{17}\Delta$ were 0.004‰, 0.2‰ and 8 per meg, respectively. The isotopic and O_2/Ar ratios are reported with respect to atmospheric O_2 , which is the standard of choice for isotope measurements in natural O_2 gas (Barkan & Luz 2003).

$^{17}\Delta_{\text{dis}}$ at air-seawater equilibrium ($^{17}\Delta_{\text{eq}}$). As discussed above, the value for $^{17}\Delta_{\text{eq}}$ is needed in calculating GOP using Eq. (4). Luz & Barkan (2000) determined its value at 25°C to be 16 ± 2 per meg (mean \pm SE). Later, Juranek & Quay (2005) and Sarma et al. (2006) confirmed this result, both studies measuring $^{17}\Delta_{\text{eq}}$ at room temperature to be 18 ± 2 per meg (mean \pm SE). More recently however, Reuer et al. (2007)

reported a $^{17}\Delta_{\text{eq}}$ of 8 ± 2 per meg (mean \pm SE) at both 11 and 25°C. The new value is statistically different from the previous one. Because of the importance of $^{17}\Delta_{\text{eq}}$ in calculating GOP (the GOP estimate is quite sensitive to $^{17}\Delta_{\text{eq}}$, especially in situations where $^{17}\Delta_{\text{eq}}$ and $^{17}\Delta_{\text{dis}}$ values are close), we ran more equilibrium experiments over the temperature range of 3.5 to 25°C.

The experiments were carried out in an open 3 l flask. Fresh outside air was bubbled directly through seawater poisoned with saturated HgCl_2 solution (1 ml in 100 g of water) to prevent biological activity. The water in the flask was constantly stirred and the temperature was kept constant within $\pm 0.1^\circ\text{C}$. Atmospheric pressure was monitored and variations during the experiment were <1 mm Hg. Bubbling was stopped 2 h before sampling. The time needed to reach isotopic equilibrium was determined in preliminary experiments by monitoring the changes in $\delta^{18}\text{O}$ and the O_2/Ar ratio. At steady state, both $\delta^{18}\text{O}$ and the O_2/Ar ratio agreed with a mutual experimental error, with values corresponding to those of Benson & Krause (1984) and Hamme & Emerson (2004).

RESULTS AND DISCUSSION

$^{17}\Delta_{\text{dis}}$ at air-seawater equilibrium ($^{17}\Delta_{\text{eq}}$)

The experimental results are given in Table 1, which shows the new value of $^{17}\Delta_{\text{eq}}$ at 25°C to be almost identical to our previous result (Luz & Barkan 2000). However, smaller values were obtained at lower temperatures. Based on the new measurements, $^{17}\Delta_{\text{eq}}$ can be expressed by a simple relationship: $^{17}\Delta_{\text{eq}} = 0.6 \times T + 1.8$, where T is the temperature in °C. Using this equation, we calculated $^{17}\Delta_{\text{eq}}$ at 11.2°C to be 8 per meg, which is in good agreement with the value of Reuer et al. (2007; 7 per meg); however, their value at 24.8°C (9 per meg) differs from our calculated value. We cannot explain the difference at 24.8°C, but, considering that our old and new values are in excellent agreement with the values from both Juranek & Quay (2005) and Sarma et al. (2006), and also because the scatter of the data of Reuer et al. (2007) is considerably larger (SD: ± 11 per meg) than that of ours (SD: ± 3 per meg), we conclude that our value is more accurate. Therefore, we used our new measurements of $^{17}\Delta_{\text{eq}}$ and its temperature dependence for GOP calculations in the present study.

Eilat coral reef reserve

Measurements of $^{17}\Delta_{\text{dis}}$ and $\delta\text{O}_2/\text{Ar}$ were carried out in September 1998 in the coral reef reserve near Eilat, Israel. All the data are given in Table A1 in Appen-

Table 1. $\delta^{17}\text{O}$, $\delta^{18}\text{O}$ and $^{17}\Delta$ (vs. atmospheric O_2 in ‰ and per meg, respectively) of dissolved oxygen at air-seawater equilibrium. The errors indicated for the means are 95% CIs (SEs of the mean multiplied by Student's *t*-factor)

	$\delta^{17}\text{O}$	$\delta^{18}\text{O}$	$^{17}\Delta$
3.5°C			
1	0.461	0.875	8
2	0.409	0.790	0
3	0.424	0.815	2
4	0.405	0.772	5
5	0.422	0.805	5
Average	0.424 ± 0.02	0.811 ± 0.04	4 ± 3
12.2°C			
1	0.422	0.796	9
2	0.423	0.804	7
3	0.415	0.780	11
4	0.419	0.792	9
5	0.425	0.806	8
Average	0.421 ± 0.00	0.796 ± 0.01	9 ± 2
25.0°C			
1	0.372	0.684	18
2	0.412	0.758	20
3	0.411	0.773	11
4	0.367	0.680	15
5	0.391	0.716	20
Average	0.391 ± 0.02	0.724 ± 0.05	17 ± 4

dix 1. Each data point in Table A1 represents the average of 2 determinations with a precision (absolute difference from the average) of 1‰ for $\delta\text{O}_2/\text{Ar}$, 0.02‰ for $\delta^{18}\text{O}_{\text{dis}}$ and 5 per meg for $^{17}\Delta$.

Variations with respect to time and distance from shore, starting in open waters and going through the reef and into the back-lagoon, are shown in Figs. 2 & 3. The day-to-night variations were recorded in the lagoon (20 m off shore), while the day and night results in open waters were similar and within the analytical error. The situation in the open sea (500 m off shore, Fig. 2) is similar to previous studies in the oceanic mixed layer (e.g. Luz & Barkan, 2000). The negligible diel changes in $\delta\text{O}_2/\text{Ar}$ and $^{17}\Delta$ confirm the steady state assumption in these studies. We also note that the small deviations of both $\delta\text{O}_2/\text{Ar}$ and $^{17}\Delta$ from equilibrium values suggest that gas exchange is the dominant process in the open sea.

In contrast to the open sea, the situation in the reef system is very different. The diel amplitudes in both $\delta\text{O}_2/\text{Ar}$ and $^{17}\Delta_{\text{dis}}$ (Figs. 2 & 3) clearly show that biological fluxes were very high in comparison to air-water gas exchange and water exchange between the reef system and the open sea. For the most part, these fluxes of O_2 production and consumption originate from the reef core. Effective washout by waves and currents considerably decreased the effect of the biological processes on the side of the reef that faces the

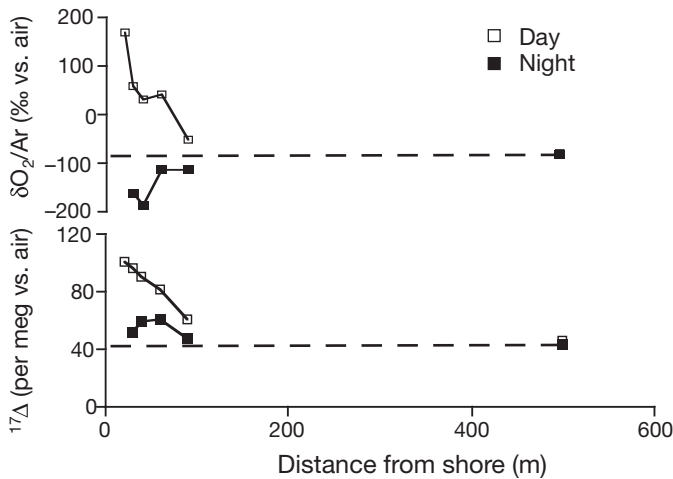


Fig. 2. Variations in $\delta O_2/Ar$ and $^{17}\Delta_{dis}$ in the Eilat coral reef reserve during the day and at night as a function of distance from the shore. The reef core is located at 40 m from the shore and the center of the back lagoon is ~ 20 m from the shore. Note that diel variations are minimal in the open sea, but are strong in the back lagoon. Dashed lines indicate open sea values

open sea, and significant exchange with open sea waters due to tides and cross-shore currents occurred even in the lagoon.

As can be seen from the variations in $\delta O_2/Ar$ in Figs. 2 & 3, photosynthesis is greater than respiration at daytime and O_2 becomes supersaturated. At night, the situation is reversed and respiratory consumption lowers O_2 levels to undersaturation. This clearly shows that, despite tides and cross-shore currents, $\delta O_2/Ar$ is significantly affected by the balance between photosynthetic production and respiratory consumption. In contrast, the situation with $^{17}\Delta_{dis}$ is different. Together

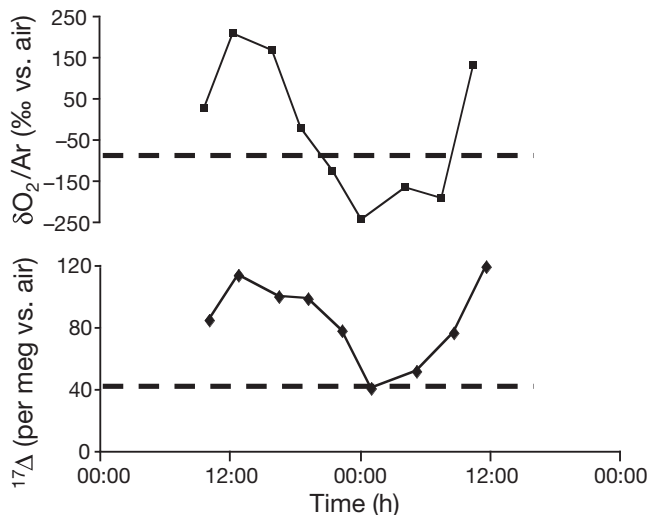


Fig. 3. Variations in $\delta O_2/Ar$ and $^{17}\Delta_{dis}$ vs. time in the back lagoon. Dashed lines indicate open sea values

with $\delta O_2/Ar$, it increases at daytime due to intense photosynthesis. However, despite the strong respiratory consumption of O_2 in the dark that lowers $\delta O_2/Ar$, the value of $^{17}\Delta_{dis}$ tends to approach that found in the open sea (~ 40 per meg) due to tides and cross-shore currents and remains unchanged by respiration. This result, obtained from the study of a real natural system, confirms our assumption that $^{17}\Delta_{dis}$ is not changed by respiration; thus, $^{17}\Delta_{dis}$ variations are useful as a measure of GOP.

Sargasso Sea

We sampled seawater in the Sargasso Sea during routine BATS cruises from March 2000 to January 2001. The BATS station is located southeast of the Bermuda islands ($31^\circ 40' N$, $64^\circ 10' W$). All data, including temperature and salinity, are given in Table A2. Each data point represents the average of 2 determinations with a precision (absolute difference from the average) of 1‰ for $\delta O_2/Ar$, 0.02‰ for $\delta^{18}O_{dis}$ and 4 per meg for $^{17}\Delta$.

Profiles of temperature, $\delta O_2/Ar$ and $^{17}\Delta_{dis}$ in October 2000 are shown in Fig. 4, while Fig. 5 shows seasonal variations in $^{17}\Delta_{dis}$. Fig. 4 illustrates a typical picture when the seasonal thermocline is present. In the mixed layer, due to effective ventilation of photosynthetic O_2 , the values of both $\delta O_2/Ar$ and $^{17}\Delta_{dis}$ are only slightly larger than in equilibrium. In the upper part of the thermocline, the deviations from equilibrium for both parameters are much larger. In the lower part of the thermocline (below 100 m), the picture becomes very different: $\delta O_2/Ar$ values are well below equilibrium, whereas $^{17}\Delta_{dis}$ remains well above equilibrium with air (~ 16 per meg for conditions near Bermuda). Similar relationships were also observed at much greater depth (2000 m, Table A2).

As noted previously (Jenkins & Goldman 1985, Spitzer & Jenkins 1989), the $\delta O_2/Ar$ maximum in the thermocline originates from the seasonal net accumulation of photosynthetic O_2 , which is possible due to the attenuation of vertical mixing caused by density stratification in the thermocline. In the aphotic zone, $\delta O_2/Ar$ values are smaller than equilibrium values, probably indicating the dominance of respiration or entrainment of undersaturated water either vertically or horizontally.

The behavior of $^{17}\Delta_{dis}$ in the seasonal thermocline is different. In the photic zone, it reaches a maximum due to accumulation of photosynthetic O_2 production. Some of the newly produced O_2 is probably transported to the aphotic zone by diapycnal mixing, where $^{17}\Delta_{dis}$ keeps accumulating despite O_2 consumption. We note that some of the accumulation in the aphotic zone

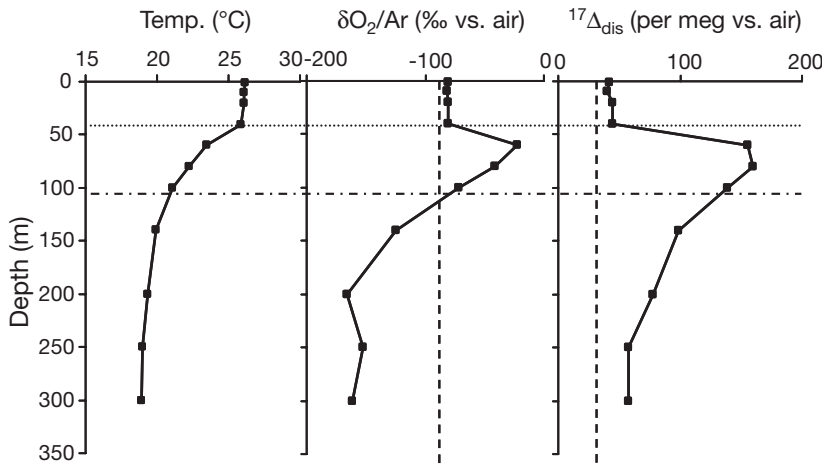


Fig. 4. Temperature, $\delta O_2/Ar$ and $^{17}\Delta_{dis}$ profiles at the Bermuda Atlantic Time-series Study (BATS) station in October 2000. Vertical dashed lines: gas exchange equilibrium; dotted horizontal line: depth of the bottom of the mixed layer; and dashed dotted horizontal line: depth of penetration of 1% of surface radiation

may not be strictly from vertical transport but may also be derived from the photic zone elsewhere. Regardless of the exact location of the source photic zone, this is another example of the unique behavior of $^{17}\Delta_{dis}$. It can increase due to GOP, it can be reset to its equilibrium value by air–sea gas exchange, but it is not affected by respiration.

The seasonal accumulation of $^{17}\Delta_{dis}$ is demonstrated in Fig. 5. Starting in March, the upper ocean is well mixed and $^{17}\Delta_{dis}$ is relatively uniform down to 300 m.

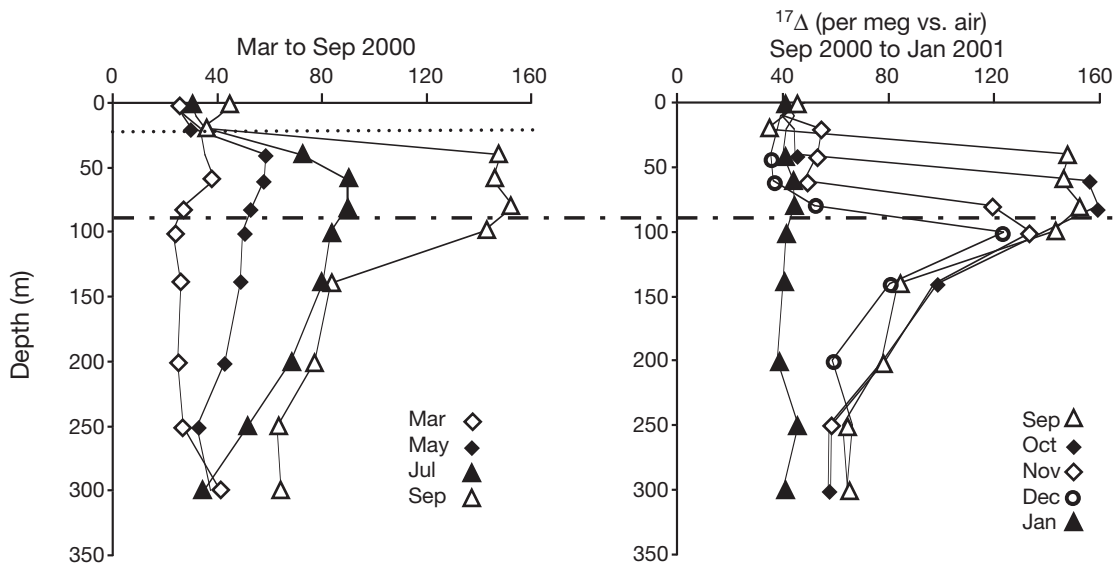


Fig. 5. Seasonal variations in $^{17}\Delta_{dis}$ at the Bermuda Atlantic Time-series Study (BATS) station. (.....) Approximate depth of the bottom of the summer mixed layer. From October to January, the mixed layer deepens and its bottom is found approximately at the depth where $^{17}\Delta_{dis}$ starts to increase sharply. (- - -) Average depth of penetration of 1% of surface radiation. Note the accumulation of the $^{17}\Delta_{dis}$ signal both in the euphotic zone and at depths where light levels are below 1% of surface radiation

With the formation of the seasonal thermocline, ventilation becomes confined to the shallow mixed layer where $^{17}\Delta_{dis}$ is only slightly greater than $^{17}\Delta_{eq}$. In the thermocline, contrasting accumulation of photosynthetic O_2 is clearly evident from the increasing $^{17}\Delta_{dis}$ values. Buildup of the seasonal maximum continues until September. In October, the upper part of the summer $^{17}\Delta$ maximum starts to erode due to the cooling and deepening of the mixed layer. Further cooling continues to erode the maximum in November and December and a complete reset is observed in January. Despite respiration, the shape of the curves below the mixed layer remains relatively constant. This again shows that $^{17}\Delta_{dis}$ is not affected by respiration and can be reset only by ventilation and mixing. Hence, $^{17}\Delta_{dis}$ accumulation can be used to calculate the overall rate of photosynthesis below the mixed layer.

Before calculating the seasonal O_2 budget, it is important to note that the $^{17}\Delta_{dis}$ signal, which accumulates in the thermocline, is distributed over the photic zone as well as in the upper part of the aphotic zone, where there is no photosynthesis. In the calculation of the O_2 budget, we assume that the accumulation in the aphotic zone resulted only from GOP in the overlying layers. This accumulation reflects mixing of water from

the photic zone to the deeper dark ocean and vice versa. In their study of profiles in the Pacific Ocean, Hendricks et al. (2005) suggested that some of this accumulation may be the result of lateral isopycnal mixing originating from remote regions. However, horizontal gradients of most tracer properties in the oligotrophic ocean are typically small, and advection effects are thus likely to be small. For example, Emerson et al. (1995) showed in their study of the subtropical Pacific Ocean that gas transport by isopycnal flow is very small.

Our calculations were done separately for the mixed layer and the seasonal thermocline. While we can determine instantaneous rates from $^{17}\Delta_{\text{dis}}$ using Eq. (4) for the mixed layer, we can only determine average rates for a given time period for the thermocline. Furthermore, Eq. (4) is suitable only for a steady state under the simplifying assumption that there is no interaction between the mixed layer and the thermocline. Clearly, this simplification is not justified for the period when the thermocline erodes due to surface cooling and 'old' seawater is introduced into the mixed layer. For this reason, we calculated GOP only for the period from May to October, during which a strong thermocline separates the mixed layer from the deep water. The chosen period is also the warming period when vertical advection of water and turbulent diffusion across the base of the mixed layer are negligible (see Emerson 1987 and references therein). Sarma et al. (2005) mentioned that the steady state assumption might be violated if wind speed varies rapidly over several days. We carefully analyzed the wind speeds for the chosen period and did not observe such changes. Overall, we can suggest with a high degree of probability that the mixed layer was at a quasi-steady state.

O₂ budget in the mixed layer

The instantaneous GOP rates in the mixed layer are given in Table 2, while the integrated GOP rates for 3 periods are shown in Table 3. We also present the NOP rates calculated using Eq. (2). We estimated the uncertainties for both GOP and NOP as 30%, reflecting uncertainties in piston velocity, $^{17}\Delta_{\text{dis}}$ and $^{17}\Delta_{\text{eq}}$. The NOP/GOP ratio was high in May (0.21), decreased in July (0.12) and remained practically constant until November (0.08). The small NOP/GOP fractions clearly indicate that most of the O₂ produced in the mixed layer was recycled by respiratory consumption mechanisms.

Table 2. Estimates of instantaneous NOP, GOP (mmol O₂ m⁻² d⁻¹) and P(¹⁴C) (mmol C m⁻² d⁻¹) in the mixed layer at the Bermuda Atlantic Time-series (BATS) station. NOP: net O₂ production; GOP: gross O₂ production; P(¹⁴C): production based on ¹⁴C fixation data from BATS (ftp.bbsr.edu/bats/); *k*: piston velocity, values calculated from wind speeds using the relationship of Wanninkhof (1992). Wind speed data were taken from the Bermuda Weather Service. We first calculated an averaged *k* value for a given day and then used the daily values for calculating monthly averages. Numerical tests have shown that the different schemes of averaging monthly piston velocity led to similar results, and we estimated the total error in *k* to be 25%

	08 May 00	10 Jul 00	11 Sept 00	16 Oct 00
C _o (mmol m ⁻³)	216.9	199.7	194.9	201
<i>k</i> (m d ⁻¹)	2.7	3	2.2	4.4
δO ₂ /Ar (δ)	-79.6	-80.9	-77.6	-80.6
¹⁷ Δ _{dis} (per meg)	27	32	40	40
NOP	6	5.3	5.4	8.3
GOP	28.8	45.3	49.7	102.7
P(¹⁴ C)	8.3	8.9	6.3	13.5
GOP/P(¹⁴ C)	3.5	5.1	7.9	7.6
NOP/GOP	0.21	0.12	0.11	0.08
P(¹⁴ C)/NOP	1.38	1.68	1.17	1.63

The NOP/GOP ratio (*f*_{O₂}) is analogous to the commonly used *f*-ratio between net and gross production in other studies (e.g. Eppley & Peterson 1979). However, in our study this ratio is based on rates of O₂ production and consumption from comparable sets of field measurements, rather than on comparison of separate estimates of ¹⁵N and ¹⁴C fixation rates. As in other studies, it provides information on the ability of an ecosystem to retain, rather than to rapidly recycle, organic matter and sets an upper limit for the amount of production that can be exported from the euphotic zone. A high *f*_{O₂}-ratio indicates high NOP for a given rate of gross photosynthesis, whereas a lower ratio indicates that most of the newly produced O₂ is consumed in the upper layers.

We note that *f*_{O₂}-ratios may differ from production values calculated based on ¹⁵N and ¹⁴C. We emphasize

Table 3. Estimates of GOP (mmol O₂ m⁻² d⁻¹) and P(¹⁴C) (mmol C m⁻² d⁻¹) at the BATS station. Values in the mixed layer are averages calculated from the rates at the beginning and end of each period. Abbreviations are as indicated in Table 2

Period	Mixed layer		Thermocline		% production in the thermocline	
	GOP	P(¹⁴ C)	GOP	P(¹⁴ C) ^a	GOP	P(¹⁴ C)
May – July	37.1	8.6	112.8	34.5	75	80
July – Sept	47.5	7.6	144.9	27.7	75	78
Sept – Oct	76.2	9.9	74.1	15.2	49	61

^aDepth-integrated P(¹⁴C) rates were determined using a trapezoidal integration

that rapid recycling of O_2 between photosynthesis and respiratory mechanisms does not imply similar recycling of carbon. The difference in f -ratios is partly related to O/C quotients in respiration and photosynthesis (e.g. Redfield ratios). This is reflected in the different ratios of NOP and net carbon production (NCP) rates, with the NOP/NCP ratio being ~ 1.4 (see Laws 1991). However, a much greater difference between GOP and gross carbon fixation rates may be expected due to consumption of O_2 by the Mehler reaction and chlororespiration. For example, we demonstrated recycling of $\sim 40\%$ of photosynthetic O_2 by such mechanisms in rapidly growing cultures (Helman et al. 2005). Much higher rates of recycling may be expected under natural conditions not as favorable to growth as in our laboratory experiments.

From the above discussion, it is clear that gross production rates of carbon and O_2 should be compared with caution, and we don't know whether constant ratios should be expected in the ocean. Thus, we compared our results only with O_2 -based estimates of f -ratios. In such comparisons, similar or even smaller f_{O_2} -ratios were observed during the termination of the spring diatom bloom on the west Florida shelf (Hitchcock et al. 2000), in the oligotrophic offshore regions of the Arabian Sea (Dickson et al. 2001) and during the austral summer across the Antarctic Polar Front (Dickson & Orcharado 2001). In contrast, much higher values (0.3 to 0.5) were obtained for upwelling events in the Arabian Sea (Dickson et al. 2001), the equatorial Pacific (Bender et al. 1999), the North Atlantic spring bloom (Bender et al. 1992, Kiddon et al. 1993) and the Pacific sector of the Southern Ocean in the Ross Sea during summer and fall (Bender et al. 2000).

In all studies mentioned above, f_{O_2} -ratios were determined from bottle incubations. However, as we showed previously (Luz et al. 2002), net production rates evaluated from bottle incubations may not be accurate. In the present study, we determined f_{O_2} -ratios only from *in situ* measurements (O_2/Ar ratio and $^{17}\Delta_{dis}$), and it is more appropriate to compare them with those of other studies that used similar methods. Our results agree well with those of Juranek & Quay (2005) from the Hawaii Ocean Time-series Station (HOTS) (~ 0.1 in summer), those of Hendricks et al. (2005) from the equatorial Pacific (average value of 0.06) and of Reuer et al. (2007) from the Southern Ocean (average of 0.13, representative of austral summer conditions). Hence, low f_{O_2} -ratios are common in many parts of the ocean.

In Table 2, we also present the corresponding rates of production based on ^{14}C fixation, $P(^{14}C)$. $P(^{14}C)$ values are much lower than GOP, but are close to NOP, which is in good agreement with previous studies (e.g. Bender et al. 1999, Luz et al. 2002, Robinson et al.

2009). Furthermore, the given period is characterized by high GOP/ $P(^{14}C)$ ratios (3 to 8). We believe that the high GOP/ $P(^{14}C)$ ratios may be a result of very rapid rates of O_2 cycling between gross production in Photosystem II and various biological uptake mechanisms. Indeed, there is a clear relationship between NOP/GOP and GOP/ $P(^{14}C)$ ratios: $GOP/P(^{14}C) = -33.0 \times NOP/GOP + 10.3$. Such rapid cycling may also indicate O_2 uptake by mechanisms involving O_2 consumption with no or little CO_2 release. The corresponding mechanisms may be photorespiration, in which O_2 uptake is $\sim 3\times$ the rate of CO_2 release, or the Mehler reaction in which there is no CO_2 release at all. Both processes notably occur only under illumination, and an important question is whether rapid carbon cycling accompanies the rapid O_2 cycling. In cases where the Mehler reaction and photorespiration, are significant, the discrepancy between estimates of primary production derived from O_2 isotope measurements and ^{14}C incubations is easily resolved. However, if the alternative is the case, i.e. a high GOP/ $P(^{14}C)$ ratio results from processes involving both O_2 uptake and CO_2 production, rapid cycling of the ^{14}C label during incubation is implied. Clearly, more research is needed in order to evaluate these possibilities.

The GOP/ $P(^{14}C)$ ratios obtained in the present study are considerably higher than the average value of 2.2 observed during the Joint Global Ocean Flux Study (JGOFS) North Atlantic Bloom Experiment, the JGOFS Equatorial Pacific Experiment and the JGOFS Arabian Sea cruises (Bender et al. 1992, 1999, Laws et al. 2000), as well as the commonly used value of 2.7 (Marra 2002). However, the high values are typical in blooms. For example, in our monthly monitoring over 2 yr in Lake Kinneret (Luz et al. 2002), the non-bloom ratio was 1.93, whereas it was 7.6 during a bloom. From JGOFS results for the Ross Sea (Bender et al. 2000, Smith et al. 2000), we calculated the GOP/ $P(^{14}C)$ ratio for peak bloom conditions as 5.5, while it was only 1.5 to 2 post bloom, when gross production was low. Finally, in the recent work of Robinson et al. (2009), the ratio was determined to be 4.8 for pre-bloom and bloom conditions in the Celtic Sea.

It should be mentioned that the GOP/ $P(^{14}C)$ ratios estimated in the above studies are based on bottle incubations. However, Juranek & Quay (2005) have shown that GOP determined using the $^{17}\Delta$ method is 1.5 to $2\times$ higher than that based on the ^{18}O bottle incubation technique. This may partly explain the difference between our estimates of the GOP/ $P(^{14}C)$ ratios and those of others. In recent years, 2 studies have reported GOP/ $P(^{14}C)$ ratios obtained using our methods: Juranek & Quay (2005) for the North Pacific subtropical gyre during winter and summer, and Reuer et al. (2007) for the Southern Ocean during the austral

summer. In the first case, the GOP/P(¹⁴C) ratio was estimated at ~2.0, which is similar to the previously reported values of 2 to 3; however, the GOP/P(¹⁴C) ratio in the second study was 5.4, in excellent agreement with our observations. Thus, overall, there is clear indication that the GOP/P(¹⁴C) ratio in the open sea may vary over wide ranges. While it is not obvious what environmental factors cause the different ratios, it is clear that there is no simple and unique relationship between GOP and P(¹⁴C).

O₂ budget in the thermocline

For the calculation in the thermocline, we assumed that, between May and October, there was neither addition nor loss of O₂ from the mixed layer above or the deep ocean below 300 m, nor lateral advection. These assumptions are consistent with our discussion above. The GOP rate (mmol O₂ m⁻² d⁻¹) between 2 observations (initial and final) was calculated as:

GOP =

$$\frac{\sum([O_2] \times ^{17}\Delta)_{\text{fin}} - \sum([O_2] \times ^{17}\Delta)_{\text{in}} + (\sum[O_2]_{\text{fin}} - \sum[O_2]_{\text{in}}) \times ^{17}\Delta_{\text{avg}}}{N \times (^{17}\Delta_{\text{max}} - ^{17}\Delta_{\text{avg}})} \quad (5)$$

where $\sum([O_2] \times ^{17}\Delta)$ is the summation of the amount of O₂ m⁻² × ¹⁷Δ_{dis} over the depth interval from the bottom of the mixed layer to 300 m; ¹⁷Δ_{avg} is the average ¹⁷Δ_{dis} for a given period; and *N* is the number of days between the initial and final observation. We note that this simple budget cannot be used for NOP because, unlike GOP, it is biased by O₂ consumption due to decomposition of exported organic particles from the photic zone in the dark part of the seasonal thermocline.

In Table 3, we present GOP rates obtained using Eq. (5) together with the corresponding rates of P(¹⁴C). As in the case of the mixed layer, GOP was 3 to 5× higher than P(¹⁴C). This shows, for the first time, that most of the newly produced O₂ in the thermocline is recycled by respiratory mechanisms. In this respect, the situation in the thermocline is very similar to that in the mixed layer.

CONCLUSIONS

Field studies in the coral reef reserve near Eilat, where biological fluxes (photosynthesis and respiration) are high in comparison to physical effects, confirm our hypothesis that (1) ¹⁷Δ of dissolved O₂ is affected by photosynthesis, ocean dynamics and air–water gas exchange, but not by respiration; (2) ¹⁷Δ_{dis} significantly increases below the oceanic mixed layer between March and September in the

North Atlantic near Bermuda, reflecting the seasonal integration of photosynthesis in the thermocline; (3) NOP/GOP ratios in the mixed layer of the Atlantic Ocean near Bermuda range from 0.08 to 0.21; and (4) up to 80 to 90 % of the newly produced O₂ are recycled by respiratory consumption mechanisms both within the mixed layer and in the seasonal thermocline.

Acknowledgements. We are grateful to the Inter-University Institute for Marine Sciences, Eilat, Israel, for infrastructure that supported the study in the coral reef. We thank J. Erez, B. Lazar and J. Silverman for help and advice in sampling in the Eilat coral reef. The work in BATS would have been impossible without the active help of the BATS team and the crew of RV 'Weather Bird II'. We also thank S. Bell for careful sampling and handling of the water samples during the BATS cruises. B. Kolts of the Bermuda Weather Service provided valuable wind speed data used for calculating piston velocities, and N. Nelson and D. Court provided data on light penetration. Comments from 3 anonymous reviewers greatly improved the manuscript. Part of this study was carried out during the 8th International Workshop of the Group for Aquatic Primary Productivity (GAP) and the Batsheva de Rothschild Seminar on Gross and Net Primary Productivity held at the Inter-University Institute for Marine Sciences, Eilat, Israel in April 2008. This research was supported by grants from the USA-Israel Binational Science Foundation and The Israel Science Foundation.

LITERATURE CITED

- Barkan E, Luz B (2003) High-precision measurements of ¹⁷O/¹⁶O and ¹⁸O/¹⁶O of O₂ and O₂/Ar ratio in air. *Rapid Commun Mass Spectrom* 17:2809–2814
- Barkan E, Luz B (2005) High precision measurements of ¹⁷O/¹⁶O and ¹⁸O/¹⁶O ratios in H₂O. *Rapid Commun Mass Spectrom* 19:3737–3742
- Bender ML, Ducklow H, Kiddon J, Marra J, Martin J (1992) The carbon balance during the 1989 spring bloom in the North Atlantic Ocean, 47° N, 20° W. *Deep-Sea Res* 39:1707–1725
- Bender ML, Orchardo J, Dickson ML, Barber R, Lindley S (1999) *In vitro* O₂ fluxes compared with ¹⁴C production and other rate terms during the JGOFS Equatorial Pacific experiment. *Deep-Sea Res* I 46:637–654
- Bender ML, Dickson ML, Orchardo J (2000) Net and gross production in the Ross Sea as determined by incubation experiments and dissolved O₂ studies. *Deep-Sea Res* II 47:3141–3158
- Benson BB, Krause DK Jr (1984) The concentration and isotopic fractionation of oxygen dissolved in freshwater and seawater in equilibrium with atmosphere. *Limnol Oceanogr* 29:620–632
- Craig H, Hayward T (1987) Oxygen supersaturation in the ocean: biological versus physical contributions. *Science* 235:199–202
- Dickson ML, Orchardo J (2001) Oxygen production and respiration in the Antarctic Polar Front region during the austral spring and summer. *Deep-Sea Res* II 48:4101–4126
- Dickson ML, Barber RT, Marra J, McCarthy JJ, Sambrotto RN (2001) Production and respiration rate in the Arabian Sea during the 1995 northeast and southeast monsoons. *Deep-Sea Res* II 48:1199–1230

- Emerson S (1987) Seasonal oxygen cycles and biological new production in surface waters of the subarctic Pacific Ocean. *J Geophys Res* 92:6535–6544
- Emerson S, Quay P, Stump C, Wilbur D, Knox M (1991) O₂, Ar, N₂ and ²²²Rn in surface waters of the subarctic ocean: net biological O₂ production. *Global Biogeochem Cycles* 5:49–69
- Emerson S, Quay P, Stump C, Wilbur D, Shudlich R (1995) Chemical tracers of productivity and respiration in the subtropical Pacific Ocean. *J Geophys Res* 100: 15873–15887
- Eppley RW, Peterson BJ (1979) Particulate organic matter flux and planktonic new production in the deep ocean. *Nature* 282:677–680
- Guy RD, Fogel ML, Berry JA (1993) Photosynthetic fractionation of stable isotopes of oxygen and carbon. *Plant Physiol* 101:37–47
- Hamme RC, Emerson SR (2004) The solubility of neon, nitrogen and argon in distilled water and seawater. *Deep-Sea Res I* 51:1517–1528
- Helman Y, Barkan E, Eisenstadt D, Luz B, Kaplan A (2005) Fractionation of the three stable oxygen isotopes by oxygen-producing and oxygen-consuming reactions in photosynthetic organisms. *Plant Physiol* 138:2292–2298
- Hendricks MB, Bender ML, Barnett BA (2004) Net and gross O₂ production in the southern ocean from measurements of biological O₂ saturation and its triple isotope composition. *Deep-Sea Res I* 51:1541–1561
- Hendricks MB, Bender ML, Barnett BA, Strutton P, Chavez FP (2005) Triple oxygen isotope composition of dissolved O₂ in the equatorial Pacific: a tracer of mixing, production, and respiration. *J Geophys Res* 110:C12021.1–C12021.17 doi:10.1029/2004JC002735
- Hitchcock GL, Vargo GA, Dickson ML (2000) Plankton community composition, production and respiration in relation to dissolved inorganic carbon on the West Florida Shelf, April 1996. *J Geophys Res* 105:6579–6589
- Jenkins WJ, Goldman JC (1985) Seasonal oxygen cycling and primary production in the Sargasso Sea. *J Mar Res* 43: 465–491
- Juranek LW, Quay PD (2005) *In vitro* and *in situ* gross primary and net community production in the North Pacific subtropical gyre using labeled and natural abundance isotopes of dissolved O₂. *Global Biogeochem Cycles* 19: GB3009. doi:10.1029/2004GB002384
- Kiddon J, Bender ML, Orchardo J, Caron DA, Goldman JC, Dennett M (1993) Isotopic respiration of oxygen by respiring marine organisms. *Global Biogeochem Cycles* 7: 679–694
- Laws EA (1991) Photosynthetic quotients, new production and net community production in the open ocean. *Deep-Sea Res* 38:143–167
- Laws EA, Landry MR, Barber RT, Campbell L, Dickson ML, Marra J (2000) Carbon cycling in primary production bottle incubations: inferences from grazing experiments and photosynthetic studies using ¹⁴C and ¹⁸O in the Arabian Sea. *Deep-Sea Res II* 47:1339–1352
- Luz B, Barkan E (2000) Assessment of oceanic productivity with the triple-isotope composition of dissolved oxygen. *Science* 288:2028–2031
- Luz B, Barkan E (2005) The isotopic ratios ¹⁷O/¹⁶O and ¹⁸O/¹⁶O in molecular oxygen and their significance in biogeochemistry. *Geochim Cosmochim Acta* 69:1099–1110
- Luz B, Barkan E, Bender ML, Thieme MH, Boering KA (1999) Triple-isotope composition of atmospheric oxygen as a tracer of biosphere productivity. *Nature* 400:547–550
- Luz B, Barkan E, Sagi Y, Yacobi YZ (2002) Evaluation of community respiratory mechanisms with oxygen isotopes: a case study in Lake Kinneret. *Limnol Oceanogr* 47:33–42
- Marra J (2002) Approaches to the measurement of plankton production. In: Williams PJL, Thomas DN, Reynolds CS (eds) *Phytoplankton productivity: carbon assimilation in marine and freshwater ecosystems*. Blackwell, Malden, MA, p 78–108
- Quay PD, Emerson S, Wilbur DO, Stump C (1993) The δ¹⁸O of dissolved O₂ in the surface waters of the subarctic Pacific: a tracer of biological productivity. *J Geophys Res* 98: 8447–8458
- Reuer MK, Barnett BA, Benders ML, Falkowskib PG, Hendricks MB (2007) New estimates of Southern Ocean biological production rates from O₂/Ar ratios and the triple isotope composition of O₂. *Deep-Sea Res I* 54:951–974
- Robinson C, Tilstone GH, Rees AP, Smyth TJ and others (2009) Comparison of *in vitro* and *in situ* plankton production determinations. *Aquat Microb Ecol* 54:13–34
- Sarma VVSS, Abe O, Hashimoto S, Hinuma A, Saino T (2005) Seasonal variations in triple oxygen isotopes and gross oxygen production in the Sagami Bay, central Japan. *Limnol Oceanogr* 50:544–552
- Sarma VVSS, Abe O, Yoshida N, Saino T (2006) Continuous shipboard sampling system for determination of triple oxygen isotopes and O₂/Ar ratio by dual-inlet mass spectrometry. *Rapid Commun Mass Spectrom* 20:3503–3508
- Sarma VVSS, Abe O, Yoshida N, Saino T (2008) Spatial variations in time-integrated plankton metabolic rates in Sagami Bay using triple oxygen isotopes and O₂:Ar ratios. *Limnol Oceanogr* 53:1776–1783
- Smith WO, Marra J, Hiscock MR, Barber RT (2000) The seasonal cycles of phytoplankton biomass and primary productivity in the Ross Sea. *Deep-Sea Res II* 47:3119–3140
- Spitzer WS, Jenkins WJ (1989) Rates of vertical mixing, gas exchange and new production: estimates from seasonal gas cycles in the upper ocean near Bermuda. *J Mar Res* 47:169–196
- Wanninkhof R (1992) Relationship between wind speed and gas exchange over the ocean. *J Geophys Res* 97: 7373–7382

Appendix 1. Summary of $\delta^{18}\text{O}$ and $^{17}\Delta$ of dissolved O₂, and $\delta\text{O}_2/\text{Ar}$ values in the Eilat reef and the Bermuda Atlantic Time-series Study (BATS) station.

Table A1. Summary of $\delta^{18}\text{O}$ and $^{17}\Delta$ of dissolved oxygen (vs. air O₂ in ‰ and per meg, respectively) and $\delta\text{O}_2/\text{Ar}$ (in ‰ vs. air O₂) in the Eilat reef

Distance from shore	Date	Time (hh:mm)	$\delta\text{O}_2/\text{Ar}$	$\delta^{18}\text{O}$	$^{17}\Delta$
20	16 Sept 98	10:00	27.3	-2.290	85
		12:40	210.5	-4.223	114
		16:25	170.3	-3.549	101
		19:12	-21.0	-1.439	99
		22:15	-124.7	0.121	78
	17 Sept 98	1:00	-241.2	2.062	41
		5:05	-163.0	1.156	52
		8:35	-190.7	-0.239	77
		11:35	130.1	-4.688	119
		16 Sept 98	16:25	59.5	-2.174
30	17 Sept 98	5:05	-184.7	1.338	60
	16 Sept 98	16:21	31.9	-1.768	90
40	17 Sept 98	5:08	-115.1	0.721	61
	16 Sept 98	16:21	42.1	-1.888	82
60	17 Sept 98	5:08	-130.4	0.867	45
	16 Sept 98	16:12	-46.0	-0.254	65
90	16 Sept 98	16:14	-59.1	-0.072	57
		17 Sept 98	5:11	-115.2	0.680
	5:11	-97.0	0.542	67	
	16 Sept 98	16:00	-80.4	0.527	41
		16:00	-80.9	0.490	52
17 Sept 98	5:18	-83.8	0.508	43	

Table A2. Summary of $\delta^{18}\text{O}$ and $^{17}\Delta$ of dissolved oxygen (vs. air O₂ in ‰ and per meg, respectively), $\delta\text{O}_2/\text{Ar}$ (in ‰ vs. air O₂), temperature (T, °C), salinity (S) and density (σ_θ) at the BATS station (the values of T and S were taken from <http://bats.bios.edu>)

Depth (m)	T	S	σ_θ	$\delta\text{O}_2/\text{Ar}$	$\delta^{18}\text{O}$	$^{17}\Delta$
Cruise no. 138, 13 March 2000						
1	19.34	36.640	26.189	-73.09	0.29	23
10	19.27	36.640	26.208	-74.5	0.23	28
20	19.25	36.641	26.214	-75.0	0.22	33
40	19.24	36.640	26.216	-73.3	0.22	35
60	19.18	36.634	26.228	-76.3	0.23	39
80	19.09	36.631	26.250	-108.2	1.02	27
100	19.08	36.631	26.253	-108.4	0.96	23
140	19.08	36.630	26.255	-110.5	0.97	26
200	19.06	36.625	26.259	-111.1	0.94	25
250	19.05	36.622	26.261	-108.5	0.87	27
300	18.38	36.541	26.371	-231.0	2.54	41
2000	3.65	34.971	27.813	-230.4	2.67	37
Cruise no. 140, 08 May 2000						
1	22.01	36.587	25.422	-80.0	0.60	24
10	21.62	36.602	25.545	-78.8	0.62	27
20	21.45	36.610	25.597	-79.8	0.65	30
40	20.39	36.628	25.903	-58.5	0.31	59
60	19.63	36.637	26.113	-65.2	0.27	58
80	19.30	36.635	26.199	-118.7	1.16	53
100	19.20	36.637	26.228	-119.2	1.42	50
140	19.17	36.636	26.235	-120.7	1.46	49
200	19.14	36.632	26.243	-122.4	1.28	43
250	19.02	36.618	26.266	-123.5	1.32	32
300	18.97	36.610	26.270	-122.6	1.32	37
2000	3.78	34.968	27.813	-243.1	2.97	38

Table A2. continued

Cruise no. 142, 10 July 2000						
1	26.51	36.465	23.981	-80.8	0.54	30
10	26.49	36.465	23.985	-81.8	0.54	32
20	26.45	36.473	24.006	-80.0	0.52	35
40	24.31	36.512	24.704	-62.2	0.25	72
60	22.57	36.577	25.263	-68.4	0.23	90
80	22.13	36.702	25.480	-105.8	0.56	90
100	21.45	36.669	25.647	-113.3	0.77	83
140	19.97	36.626	26.019	-112.3	1.18	80
200	19.05	36.619	26.256	-150.1	1.63	68
250	18.94	36.623	26.291	-140.5	1.76	52
300	18.77	36.591	26.301	-152.6	1.89	35
2000	3.62	34.948	27.800	-228.4	2.75	40
Cruise no. 144, 11 September 2000						
1	27.84	36.147	23.313	0.36	-76.5	46
10	27.91	36.457	23.523	0.46	-79.0	40
20	28.05	36.612	23.594	0.41	-77.2	34
40	25.22	36.605	24.492	0.22	-34.8	148
60	22.99	36.744	25.265	0.18	-60.4	145
80	21.76	36.737	25.613	0.34	-74.5	153
100	20.84	36.703	25.841	0.68	-104.9	142
140	19.74	36.677	26.120	1.43	-134.0	83
200	19.08	36.634	26.261	2.04	-157.8	77
250	18.82	36.578	26.286	2.10	-163.3	63
300	18.67	36.586	26.334	1.63	-151.8	64
2000	3.60	34.946	27.800	2.55	-215.7	40
Cruise no. 145, 16 October 2000						
1	26.14	36.682	24.259	0.58	-80.7	42
10	26.09	36.684	24.278	0.58	-81.3	40
20	26.07	36.686	24.288	0.59	-80.4	44
40	25.86	36.716	24.376	0.56	-80.1	45
60	23.48	36.843	25.196	0.28	-22.2	156
80	22.23	36.797	25.525	0.37	-40.7	159
100	21.08	36.754	25.815	0.58	-71.2	139
140	19.94	36.687	26.073	1.29	-124.6	98
200	19.32	36.625	26.193	2.22	-165.8	78
250	19.01	36.603	26.257	1.99	-152.2	57
300	18.92	36.591	26.273	2.16	-161.2	57
2000	3.63	34.951	27.801	2.69	-222.1	48
Cruise no. 146, 13 November 2000						
1	23.38	36.657	25.082	0.65	-82.7	39
10	23.30	36.655	25.104	0.67	-82.7	40
20	23.29	36.657	25.109	0.63	-83.4	55
40	23.30	36.66	25.111	0.65	-85.0	53
60	23.31	36.671	25.117	0.60	-82.3	48
80	22.12	36.651	25.444	0.56	-73.7	119
100	20.10	36.630	25.986	0.97	-108.4	134
140	19.09	36.586	26.218	2.50	-182.0	97
200	18.67	36.563	26.311	2.53	-179.9	79
250	18.48	36.556	26.357	2.68	-189.3	59
300	18.19	36.525	26.408	2.71	-216.7	58
2000	3.52	34.947	27.809	2.72	-222.6	37
Cruise no. 147, 11 December 2000						
1	22.01	36.600	25.433	-81.7	-0.04	48
10	22.00	36.599	25.434	-92.3	0.77	39
20	22.00	36.597	25.436	-91.7	0.70	38
40	21.94	36.588	25.445	-93.0	0.72	35
60	21.94	36.584	25.443	-92.8	0.75	36
80	21.85	36.572	25.461	-93.6	0.76	52
100	20.23	36.660	25.974	-128.3	1.30	124
140	19.23	36.613	26.203	-184.4	2.41	81

Table A2. continued

200	18.83	36.595	26.294	-176.8	2.57	59
250	18.63	36.581	26.338	-173.1	2.40	66
300	18.51	36.568	26.359	-181.5	2.52	64
2000	3.67	34.985	27.824	-247.0	2.81	44
Cruise no. 148, 25 January 2001						
1	20.16	36.606	25.947	-95.9	0.78	41
10	20.14	36.605	25.949	-97.0	0.81	44
20	20.14	36.605	25.953	-97.4	0.80	41
40	20.14	36.605	25.954	-98.2	0.79	40
60	20.13	36.604	25.955	-99.2	0.78	44
80	20.13	36.606	25.958	-97.6	0.81	44
100	20.13	36.607	25.961	-99.1	0.80	41
140	19.90	36.615	26.028	-135.7	0.79	40
200	18.72	36.575	26.307	-187.6	2.68	38
250	18.52	36.560	26.348	-193.2	2.81	46
300	18.38	36.555	26.383	-187.7	2.67	40
2000	3.64	34.976	27.816	-229.9	2.80	38

*Editorial responsibility: Tom Berman,
Migdal, Israel*

*Submitted: August 5, 2008; Accepted: March 6, 2009
Proofs received from author(s): May 11, 2009*